Contemporary Mathematics

Persistent Homology — a Survey

Herbert Edelsbrunner and John Harer

ABSTRACT. Persistent homology is an algebraic tool for measuring topological features of shapes and functions. It casts the multi-scale organization we frequently observe in nature into a mathematical formalism. Here we give a record of the short history of persistent homology and present its basic concepts. Besides the mathematics we focus on algorithms and mention the various connections to applications, including to biomolecules, biological networks, data analysis, and geometric modeling.

1. Introduction

In this section, we discuss the motivation and history of persistent homology. Both are related and our account is biased toward the particular path we took to discover the concept.

Motivation. Persistent homology is an algebraic method for measuring topological features of shapes and of functions. Small size features are often categorized as noise and much work on scientific datasets is concerned with de-noising or smoothing images and other records of observation. But noise is in the eye of the beholder, and even if we agreed on the distinction, the de-noising effort would be made difficult by dependencies that frequently lead to unintended side-effects. Features come on all scale-levels and can be nested or in more complicated relationships. It thus makes sense to survey the situation before taking steps toward change. This is what persistent homology is about. This is not to say that de-noising the data is not part of the agenda, it is, but de-noising often goes beyond measuring.

History. The concept of persistence emerged independently in the work of Frosini, Ferri, and collaborators in Bologna, Italy, in the doctoral work of Robins at Boulder, Colorado, and within the biogeometry project of Edelsbrunner at Duke, North Carolina. All three developments happened roughly simultaneously with relevant discoveries spread out over a period of fifteen years or so straddling the last turn of the century.

1991 *Mathematics Subject Classification.* Primary 55N99, 68W01; Secondary 57M99, 55T05, 52-02.

Key words and phrases. Computational algebraic topology, algorithms.

The first author was supported in part by DARPA under grants HR0011-05-1-0007 and HR0011-05-0057 and by the NSF under grant DBI-06-06873.

The second author was supported in part by DARPA under grant HR0011-05-1-0007 and by the NSF under grant DBI-06-06873.

The group around Patrizio Frosini and Massimo Ferri refers to persistence of 0-dimensional homology as size theory and is motivated by the study of the natural pseudo-distance between two functions on homeomorphic topological spaces [**3, 6, 29**]. Vanessa Robins defines persistence in shape theoretic terms and uses the idea in the study of fractal sets with alpha shapes [**40**]. The concept of alpha shapes introduced in [**23**] is also at the root of the developments at Duke. Two of the crucial algebraic ingredients of persistence, simplicial filtrations and the distinction between positive and negative simplices, date back to the implementation of three-dimensional alpha shapes by Ernst Mücke [**26**] and the enhancement of the tool by the incremental Betti number algorithm of Delfinado and Edelsbrunner [**17**]. A further critical insight is the existence of a pairing in which positive simplices mark the appearance (birth) of topological features while negative simplices mark their disappearance (death). This pairing is unique and defined using homomorphisms between homology groups induced by inclusion. That this pairing also has a fast algorithm is perhaps surprising but essential to connect the mathematical ideas to the motivating practical problems. All this is described in [**24, 45**]. The algorithm is readily coded and implementations are available as part of PLEX, a package for high-dimensional data analysis.

Outline. Section 2 introduces the basic ideas of persistent homology, progressing from special to more general settings. Section 3 describes the algorithm for the filtration of a simplicial complex, formulating it as a variant of the classic Smith normal form reduction of the boundary matrices. Section 4 presents variants of the algebraic concept of persistence, including the extension to essential homology classes motivated by the computational prediction of protein interaction. Section 5 sheds light on the connection between persistence and spectral sequences. Section 6 discusses the stability of persistence which is the starting point of a number of further developments, including the study of time series data. Section 7 concludes the paper by contemplating possible future directions the research on persistent homology may take.

2. Persistence

In this section we define the key concepts that underlie the theory of persistent homology. First we introduce persistence for single variable functions. To generalize the idea we give a terse introduction to simplicial homology and refer to [**31, 37**] for more information. We illustrate persistence first for Morse functions, then for simplicial complexes, and finally for a class of functions we refer to as tame.

Single variable functions. Let $f : \mathbb{R} \to \mathbb{R}$ be a smooth function. Recall that x is a *critical point* and $f(x)$ is a *critical value* of f if $f'(x) = 0$. A critical point x is *non-degenerate* if $f''(x) \neq 0$. Suppose now that f has only non-degenerate critical points with distinct critical values. Each critical point is then either a local minimum or a local maximum. For each $t \in \mathbb{R}$ we consider the *sublevel set* $\mathbb{R}_t = f^{-1}(-\infty, t]$. As we increase t from $-\infty$, the connectivity of $\mathbb{R}_t$ remains the same except when we pass a critical value. At a local minimum the sublevel set adds a new component and at a local maximum two components merge into one.

We pair the critical points of f by the following rule. When a new component is introduced, we say that the local minimum that creates it *represents* the component. When we pass a local maximum and merge two components, we pair the maximum with the higher (younger) of the two local minima that represent the two components. The other minimum is now the representative of the component resulting from the merger. Note that critical points that are paired need not be adjacent. When x and y are paired by this

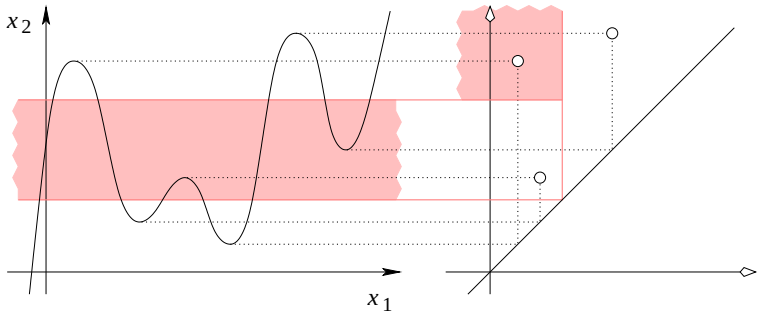

Figure 1: A single variable function with three local minima and three local maxima. The critical points are paired and each pair is displayed as a point in the persistence diagram on the right.

method we define the *persistence* of the pair to be $f(y) - f(x)$. Persistence is coded in the *persistence diagram* by mapping each pair to the point $(f(x), f(y))$ whose coordinates are the corresponding critical values. In the diagram, all points live in the half space above $x_1 = x_2$, and the persistence is easily visible as the vertical distance to this diagonal line. For reasons that will appear later, we usually adjoin the diagonal to the persistence diagram.

The remainder of this paper extends these ideas beyond single variable functions. Specifically, we extend the domain first to manifolds and then to general triangulable topological spaces. The algorithms compute homology and persistence for nested sequences of simplicial complexes which we think of as piecewise constant or piecewise linear approximations of functions defined on their underlying spaces. At the same time we extend features beyond connected components using homology which we introduce next. To go from homology to persistence we are guided by the following property we observe for the components of the sublevel sets of the single variable function $f : \mathbb{R} \to \mathbb{R}$. Let $s < t$ and consider the sublevel sets $\mathbb{R}_s \subseteq \mathbb{R}_t$. Going from s to t, components of $\mathbb{R}_s$ may merge and new components may be born and possibly merge with each other or with components of $\mathbb{R}_s$. We let $\beta_0^{s,t}$ be the number of components that are born at a finite time at or before s that belong to distinct components in $\mathbb{R}_t$. The pairing of critical points we described has the property that $\beta_0^{s,t}$ is equal to the number of pairs (x, y) with $f(x) \leq s < t < f(y)$. No other pairing satisfies this property for all $s < t$. As indicated by the shading in Figure 1, $\beta_0^{s,t}$ is also the number of points in the upper left quadrant defined by (s, t).

Homology. Let K be a simplicial complex. The $\mathbb{Z}/2\mathbb{Z}$ vector space generated by the p-dimensional simplices of K is denoted $\mathsf{C}_p(K)$. It consists of all *p-chains*, which are formal sums $c = \sum_j \gamma_j \sigma_j$, where the γ_j are 0 or 1 and the σ_j are p-simplices in K. The boundary, $\partial(\sigma_j)$, is the formal sum of the $(p-1)$-dimensional faces of σ_j and the boundary of the chain is obtained by extending ∂ linearly,

$$\partial(c) \quad = \quad \sum_j \gamma_j \partial(\sigma_j),$$

where we understand that addition is modulo 2, i.e. $1 + 1 = 0$. It is not difficult to check that $\partial \circ \partial = \partial^2 = 0$. The p-chains that have boundary 0 are called *p-cycles*. They form a subspace Z_p of C_p. The p-chains that are the boundary of $(p+1)$-chains are called *p-boundaries* and form a subspace B_p of C_p. The fact that $\partial^2 = 0$ tells us that $\mathsf{B}_p \subseteq \mathsf{Z}_p$. The

quotient group $\mathsf{H}_p(K) = \mathsf{Z}_p/\mathsf{B}_p$ is the *p-th simplicial homology group* of K with $\mathbb{Z}/2\mathbb{Z}$-coefficients. The rank of $\mathsf{H}_p(K)$ is the *k-th Betti number* of K and is denoted $\beta_p(K)$.

When we have two simplicial complexes K and L, a *simplicial map* $f : |K| \to |L|$ is continuous, takes simplices to simplices, and is linear on each. A simplicial map induces a homomorphism on homology, $\mathsf{f}_p : \mathsf{H}_p(K) \to \mathsf{H}_p(L)$, and homotopic maps induce the same homomorphism. Homotopy equivalences of spaces induce isomorphisms on homology. The simplicial approximation theorem tells us that a continuous map of simplicial complexes can be approximated by a simplicial map, so that it makes sense to talk about continuous maps inducing homomorphisms on homology.

REMARK 2.1. There are a variety of other homology theories defined in topology. Most notably *singular homology* has the advantage that it exists for arbitrary topological spaces and it is easy to define concepts like induced maps, prove that homotopy equivalent maps induce isomorphisms on homology, etc. However, in singular homology the chain groups are infinite-dimensional and therefore not directly suited to computational methods. Nevertheless, the reader should be aware of this theory. It justifies the common practice of talking about homology for spaces without an explicit triangulation. Most of the time, and certainly in low dimensions, singular and simplicial homology are equivalent theories.

Morse functions. Let $\mathbb{M}$ be a smooth manifold of dimension d and $f : \mathbb{M} \to \mathbb{R}$ a smooth function. We can imagine that $\mathbb{M}$ is embedded in $\mathbb{R}^{d+1}$ and f maps every point to its height above some hyperplane, but the reader is warned that this is not the general case as many manifolds of dimension d do not even embed in $\mathbb{R}^{d+1}$. At a *critical point* x the differential is zero, and again we call $f(x)$ a *critical value* of f. A critical point is *non-degenerate* if the *Hessian matrix* of second partial derivatives, $(\partial^2 f/\partial x_i \partial x_j)$, is non-singular. Although it takes a choice of coordinates to define this matrix, the non-singularity is independent of the choice. The *index* of a non-degenerate critical point is the number of negative eigenvalues of its Hessian; see Figure 2. A *Morse function* is a smooth function

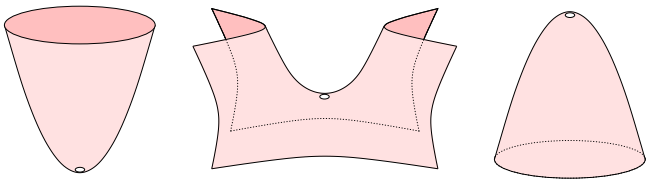

Figure 2: From left to right: a minimum, saddle, and maximum of the (vertical) height function. They are non-degenerate critical points with index 0, 1, and 2.

that has only non-degenerate critical points all of which have distinct critical values. We choose regular values $t_0 < t_1 < \ldots < t_m$ bracketing the m critical values and let $\mathbb{M}_j = f^{-1}(-\infty, t_j]$ be the *sublevel set* containing the first j critical points. Morse theory tells us that $\mathbb{M}_j$ is homotopy equivalent to the result of attaching a p-dimensional cell along its boundary to $\mathbb{M}_{j-1}$, where p is the index of the j-th critical point [**34**].

As we pass from $\mathbb{M}_{j-1}$ to $\mathbb{M}_j$ there are two possibilities for how homology might change. The first is that H_p increases rank by one, that is, $\beta_p(\mathbb{M}_j) = \beta_p(\mathbb{M}_{j-1}) + 1$. The second is that $\beta_{p-1}(\mathbb{M}_j) = \beta_{p-1}(\mathbb{M}_{j-1}) - 1$. To distinguish the two cases, we call the critical point in the first case *positive* since the sum of Betti numbers increases and the critical point in the second case *negative* since the sum of Betti numbers decreases.

Persistence gives a pairing between some of the positive critical points of index p and the negative critical points of index $p+1$. The idea is that a homology class is born at a particular time, dies at a later time, and its persistence is the difference. To make this precise, we use the maps between homology groups induced by the inclusions $\mathbb{M}_i \subseteq \mathbb{M}_j$ whenever $i \leq j$. We say a homology class α is *born at* $\mathbb{M}_i$ if it does not come from a class in $\mathbb{M}_{i-1}$. In actual fact, an entire coset is born, not just a single class. Furthermore, if α is born at $\mathbb{M}_i$ we say it *dies entering* $\mathbb{M}_j$ if the image of the map induced by $\mathbb{M}_{i-1} \subseteq \mathbb{M}_{j-1}$ does not contain the image of α but the image of the map induced by $\mathbb{M}_{i-1} \subseteq \mathbb{M}_j$ does. If α is born at $\mathbb{M}_i$ and dies entering $\mathbb{M}_j$ then we pair the corresponding critical points, x and y, and say their *persistence* is $j-i$ or $f(y)-f(x)$, depending on the application we have in mind. The latter is frequently more useful. Homology classes that are born at $\mathbb{M}_i$ and do not die are not paired by this method, but require an extension of the persistence formulation which we will describe in Section 4.

Generalizing from the case of a single variable function, persistence is coded in the *persistence diagrams*, $\mathrm{Dgm}_p(f)$, which includes the point $(f(x), f(y))$ whenever x is a positive critical point of index p that is paired with the negative critical point y of index $p+1$. As before, all points live in the half-space above the line $x_1 = x_2$ and the persistence is easily visible as the vertical distance to the diagonal. Again we adjoin the diagonal to the persistence diagram.

Simplicial complexes. Persistence can also be defined for a simplicial complex K. We recall that K is a finite set of simplices that is closed under the face relation. Two simplices are either disjoint or intersect in a common face. A *subcomplex* is a subset of simplices that is again closed under the face relation. A *filtration* of K is a nested sequence of subcomplexes that starts with the empty complex and ends with the complete complex,

$$\emptyset = K_0 \subset K_1 \subset \ldots \subset K_m = K.$$

The subcomplexes are the analog of the sublevel sets in the Morse function setting. A homology class α is *born* at K_i if it is not in the image of the map induced by the inclusion $K_{i-1} \subset K_i$. Furthermore, if α is born at K_i it *dies entering* K_j if the image of the map induced by $K_{i-1} \subset K_{j-1}$ does not contain the image of α but the image of the map induced by $K_{i-1} \subset K_j$ does. The *persistence* of α is $j-i$. As before we code the information in the persistence diagrams, one for each dimension. Each diagram is now a

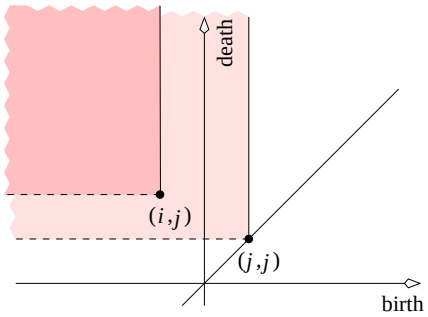

Figure 3: The number of points in the quadrant is the rank of the image of the homology group defined by the (horizontal) birth coordinate in the homology group defined by the (vertical) death coordinate.

multiset since classes can be born simultaneously and they can die simultaneously. The rank of the image of a map $\mathbf{f}_p : \mathsf{H}_p(K_i) \to \mathsf{H}_p(K_j)$ is the number of p-dimensional homology classes that are born at or before K_i and are still alive at K_j. This includes the *essential classes* of K, the ones that do not die within the filtration. It is convenient to represent an essential class born at K_i by the point (i, ∞) in the diagram. With this modification, the rank of $\operatorname{im} \mathbf{f}_p$ is the number of points of $\operatorname{Dgm}_p(K)$ in the half-open left upper quadrant $(-\infty, i] \times (j, \infty]$; see Figure 3. This is the defining property of persistence, namely that it gives the ranks of all images of maps induced by inclusion. For $i = j$ we get a quadrant anchored on the diagonal and the number of points is equal to the Betti number of K_j.

Tame functions. There are applications for which Morse functions on manifolds and filtered simplicial complexes are too limiting. We thus consider functions $f : \mathbb{X} \to \mathbb{R}$ where both the topological space $\mathbb{X}$ and the function f satisfy comparably mild conditions. As before we write $\mathbb{X}_t = f^{-1}(-\infty, t]$ for the sublevel set defined by the value t. We call f *tame* if the homology groups of every sublevel have finite ranks and there are only finitely many values t across which the homology groups are not isomorphic. Let $t_1 < t_2 < \ldots < t_m$ be these values and consider an interleaved sequence with $s_{i-1} < t_i < s_i$ for $1 \leq i \leq m$. To capture homology that exists at the beginning and at the end we set $s_{-1} = t_0 = -\infty$ and $t_{m+1} = s_{m+1} = \infty$. For each $-1 \leq i \leq j \leq m+1$ we have the inclusion $\mathbb{X}_{s_i} \subseteq \mathbb{X}_{s_j}$ and the induced homomorphism between the corresponding homology groups,

$$\mathbf{f}_p^{i,j} : \mathsf{H}_p(\mathbb{X}_{s_i}) \to \mathsf{H}_p(\mathbb{X}_{s_j}).$$

We call the image of $\mathbf{f}_p^{i,j}$ a *persistent homology group* because it consists of classes born before s_i that are still alive at s_j. The ranks of these images, $\beta_p^{i,j} = \operatorname{rank} \operatorname{im} \mathbf{f}_p^{i,j}$, are the *persistent Betti numbers* of f. By assumption, the only times at which homology classes are born or die are the t_i. Each off-diagonal point of a persistence diagram of f is therefore of the form (t_i, t_j) where $0 \leq i \leq j \leq m+1$. We can use inclusion-exclusion to determine its multiplicity,

$$\mu_p^{i,j} \quad = \quad \beta_p^{i,j-1} - \beta_p^{i-1,j-1} - \beta_p^{i,j} + \beta_p^{i-1,j}.$$

Alternatively we may use the fact that for every class that is born at t_i and dies entering t_j there is another class born at t_i that dies going to 0 at t_j. Hence $\mu_p^{i,j}$ is the rank of the *pair group*

$$\mathsf{P}_p^{i,j} \quad = \quad \frac{\operatorname{im} \mathbf{f}_p^{i,j-1} \cap \ker \mathbf{f}_p^{j-1,j}}{\operatorname{im} \mathbf{f}_p^{i-1,j-1} \cap \ker \mathbf{f}_p^{j-1,j}}.$$

With this definition the total multiplicity of points in the upper quadrant defined by (s_i, s_j) is $\beta_p^{i,j}$, as before.

A special case of a tame function is a piecewise linear function f mapping the underlying space of a simplicial complex to the real numbers. It is defined by its values at the vertices and we assume for simplicity that the restriction of f to the vertices is injective. Re-indexing the vertices such that $f(u_1) < f(u_2) < \ldots < f(u_n)$ we let K_i be the full subcomplex defined by the first i vertices. It is obtained from K_{i-1} by adding the lower star of u_i, which consists of u_i together with all simplices that connect u_i to vertices with lower function value. The nested sequence of K_i is hence referred to as the *lower star filtration* of f. We note that K_i has the same homotopy type as the sublevel set $f^{-1}(-\infty, t]$

for all $f(u_i) \leq t < f(u_{i+1})$. As far as homology is concerned, the evolution of the sublevel sets is therefore indistinguishable from the evolution of the complexes in the lower star filtration. Assuming $\mathbb{X}$ is triangulable we can approximate every tame function on $\mathbb{X}$ by a piecewise linear function on its triangulation. Using the lower star filtration we can then effectively compute the persistence diagram of this approximation. We will see in Section 6 that this diagram approximates the diagram of the tame function.

Module structure. Homology can be defined with coefficients in any abelian group. This requires orienting simplices and taking these orientations into account when defining the boundary maps, see [**31, 37**] for details. Recall that an abelian group is a *ring* if multiplication is defined and distributes over addition and it is a *field* if multiplication has an inverse. It is easy to see that persistence can then be defined using homology with coefficients in any field, $\mathbb{F}$; the definitions are the same.

Zomorodian and Carlsson [**46**] give the homology groups of K the structure of a module over the polynomial ring $\mathsf{R} = \mathbb{F}[t]$. To describe this, we recall that $\mathbb{F}[t]$ is the ring of all polynomials in the variable t with coefficients in $\mathbb{F}$. A *module* M over R is an abelian group together with an action of R on M given by $(r, m) \to rm$ that distributes over the group structure of M. When R is a field a module is better known as a vector space. A subset of R is called an *ideal* if it is a subgroup under addition and satisfies the property that for every $r \in \mathsf{R}$ and each x in the subgroup rx is again in the subgroup. For example, the even integers form an ideal in the ring of integers. An ideal is *principle* if it is generated by a single element. A *principle ideal domain* is a ring in which every ideal is principle. A standard result from commutative algebra says that $\mathbb{F}[t]$ is a principle ideal domain. Note, however, that this is false for polynomial rings in more than one variable. Finitely generated modules over principle ideal domains are easy to classify. There is a structure theorem that says that if M is such a finitely generated module then M is the direct sum of a finitely generated free module and a torsion module. Furthermore, the torsion module, $\mathsf{T}(\mathsf{M})$, is the direct sum of modules $\mathsf{T}_q(\mathsf{M})$, where the sum is over prime ideals q of R and

$$\mathsf{T}_q(\mathsf{M}) \quad = \quad \mathsf{R}/q^{l_1} \oplus \mathsf{R}/q^{l_2} \oplus \cdots \oplus \mathsf{R}/q^{l_s},$$

where $l_1 < l_2 < \ldots < l_s$. Given a filtration of complexes K_0 to K_m, as before, we form

$$\mathsf{M} \quad = \quad \mathsf{H}_p(K_0) \oplus \mathsf{H}_p(K_1) \oplus \cdots \oplus \mathsf{H}_p(K_m),$$

all with coefficients from the field $\mathbb{F}$. Let $\mathbf{f}_i^j : \mathsf{H}_p(K_i) \to \mathsf{H}_p(K_j)$ be induced by inclusion, $i \leq j$. There is then an action of $\mathbb{F}[t]$ on M given by setting $t^k\alpha = \mathbf{f}_i^{k+i}(\alpha)$ for each $\alpha \in \mathsf{H}_p(K_i)$, and this makes M a finitely generated $\mathbb{F}[t]$ module. In fact, M is called a *graded module* because of the direct summand decomposition (the grading) and the fact that t^i maps the p-graded part to the $(p+i)$-graded part. When a class α is born at K_i but does not die, it generates a free module of the form $\mathsf{R}\alpha$. When a class α is born at K_i and dies at K_j it generates a torsion module of the form $\mathsf{R}\alpha/t^{j-i}(\alpha)$, so the module structure codes persistent homology. Zomorodian and Carlsson go further to observe that the chain complexes of the K_i can also be treated as graded modules. One can then take the homology of the direct sum of all $\mathsf{C}_p(K_i)$ with coefficients in the polynomial ring, and this homology is easily identified with the persistent homology of the filtration. We refer the interested reader to [**46**] for more details.

3. Algorithm

In this section we give an algorithm to compute Betti numbers and persistence. We begin with a brief description of the classic Smith normal form algorithm; see also [**37**]. The

persistence algorithm is based on the same principles but places priority on the ordering of the simplices. Its sparse matrix implementation is particularly efficient in practice.

Smith normal form. Let K be a simplicial complex with its p-dimensional simplices indexed consecutively from 1 to $n_p = \operatorname{rank} \mathsf{C}_p$, for each dimension p. The *boundary matrices* record the face relationship for simplices whose dimensions differ by one. Specifically, $D_p[i,j] = 1$ if the i-th $(p-1)$-simplex is a face of the j-th p-simplex and $D_p[i,j] = 0$ otherwise. The Betti numbers of K can be computed from the ranks of the boundary matrices, namely $\operatorname{rank} \mathsf{B}_{p-1} = \operatorname{rank} D_p$, $\operatorname{rank} \mathsf{Z}_p = n_p - \operatorname{rank} D_p$, and therefore

$$\beta_p(K) \quad = \quad n_p - \operatorname{rank} D_p - \operatorname{rank} D_{p+1}.$$

To compute the ranks we may use elementary row and column operations. For modulo 2 arithmetic it takes time cubic in the number of simplices to reduce the boundary matrices to *Smith normal form* in which all entries are 0 except in an initial piece of the diagonal where they are 1; see Figure 4.

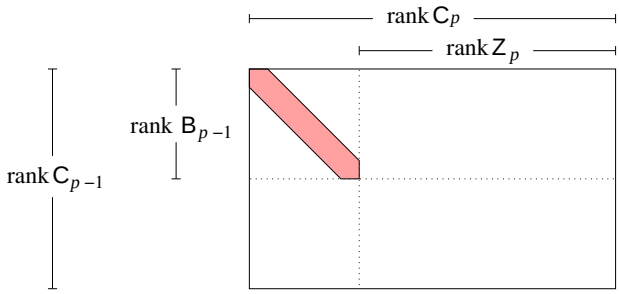

Figure 4: Smith normal form of the boundary matrix recording the face relationship between simplices of dimension p and $p-1$. Entries in the shaded portion of the diagonal are 1.

REMARK 3.1. For integer coefficients the reduction is complicated by the need to factor numbers into primes. The normal form is similar except that entries in the initial portion of the diagonal can be larger than 1. They encode torsion, which arises for $\mathbb{Z}$ but not for $\mathbb{Z}/2\mathbb{Z}$. With this change the running time of the reduction algorithm may no longer be polynomial in the size of the input. However, it can be modified to run in polynomial time [**32**]; see also [**43**].

Persistence pairing. If, in addition to the Betti numbers, we wish to compute the persistent pairing we need to be sensitive to the ordering of the simplices. We begin with a filtration of the complex, $\emptyset = K_0 \subset K_1 \subset \ldots \subset K_m = K$, and sort the simplices to get a compatible total ordering of the simplices in K, $\sigma_1, \sigma_2, \ldots, \sigma_n$. Compatible means that

- the simplices in each complex K_l in the filtration precede the ones in $K - K_l$;
- the faces of a simplex precede the simplex.

Instead of parceling out the face relation we do the computations wholesale on the combined *boundary matrix* defined by $D[i,j] = 1$ if σ_i is a codimension 1 face of σ_j and $D[i,j] = 0$ otherwise. We restrict ourselves to column additions. Let $low(j)$ be the row number of the lowest non-zero entry in column j, where we set $low(j) = 0$ if the entire

column is zero. We call D *reduced* if the restriction of low to its non-zero columns is injective, that is, each row has at most one entry that is the lowest 1 for a column. To reduce D we proceed from left to right and expand the reduced submatrix one column at a time.

```
for j = 1 to n do
  while ∃j' < j with low(j') = low(j) ≠ 0 do
    add column j' to column j
  endwhile
endfor.
```

Adding column j' decreases $low(j)$ which implies that the algorithm terminates after at most n^2 column operation. The running time is at most cubic in the number of simplices.

To read the Betti numbers off the reduced boundary matrix, R, we write $\#Zero_p(R)$ for the number of zero columns that correspond to p-simplices and $\#Low_p(R)$ for the number of lowest ones in rows that correspond to p-simplices. The rank of D is the same as that of R, namely the total number of lowest ones. Hence $\operatorname{rank} \mathsf{B}_{p-1} = \operatorname{rank} D_p = \#Low_{p-1}(R)$ and $\operatorname{rank} \mathsf{Z}_p = n_p - \operatorname{rank} D_p = \#Zero_p(R)$ since every non-zero column has a lowest one. It follows that

$$\operatorname{rank} \mathsf{H}_p(K) \quad = \quad \#Zero_p(R) - \#Low_p(R).$$

It is similarly easy to get the persistence pairs. If $low(j) = i > 0$ then σ_j is a negative simplex paired with the positive σ_i. If $low(j) = 0$ then σ_j is itself positive and we look to row j to see whether it is paired. If there is no k with $low(k) = j$ then σ_j represents an essential cycle and these generate the homology of K.

Generating cycles. If we are interested in the cycles that represent the homology classes we can track which columns are added to which. Adding column j' to column j is the same as adding the chain represented by the former to the chain represented by the latter column. The first such addition adds two simplices so that column j corresponds to $\sigma_j + \sigma_{j'}$. Subsequence additions may add other simplices but the youngest of them is always σ_j since we only add columns left to right. To do the tracking note that the

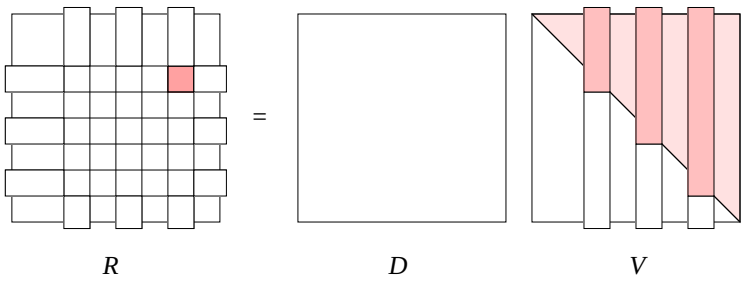

Figure 5: Shading indicates lowest non-zero entries in R and possibly non-zero entries in V. From left to right, the highlighted columns in V store an inessential cycle, an essential cycle, and a chain killing a cycle.

operation corresponds to multiplying D on the right by the *elementary matrix* that is equal to the n-by-n identity matrix except that the entry (j', j) is 1 rather than 0. Performing the column operations to reduce D thus amounts to multiplying D on the right by a matrix V, the product of the corresponding elementary matrices. Since we always add columns left to

right, V is upper triangular with ones on the diagonal. Letting R be the reduced boundary matrix we thus have $R = DV$. The columns of V give the cycles, which may be essential or inessential, and the chains that kill cycles of one lower dimension; see Figure 5. The killed cycles are boundaries and are represented by the non-zero columns in R. Since V is invertible we also have $D = RU$, with $U = V^{-1}$, in which U is again upper triangular and invertible. Similar to V the columns of U represent the cycles and chains but now in the basis represented by R.

The matrices U and V are not unique and neither is the reduced matrix R even though the pairing defined by low is unique. In some situations it is desirable to have a canonical set of cycles generating the homology groups of the K_i, one that is determined by the filtration and not the algorithm used to compute persistence [**27**]. Such a canonical set can be obtained by performing additional left to right column additions until each lowest 1 is the last 1 in its row.

Sparse matrix implementation. The initial boundary matrix is sparse by definition. Although the reduced matrix can be dense [**36**] it rarely is and using a sparse matrix data structure can lead to significant efficiency gains. We describe the particular implementation given in the original paper on persistence [**24**].

The data structure consists of a linear array, $L[1..n]$, storing a linked list with each simplex. Initially, all lists are empty and at least half the lists remain this way. Each linked list stores a cycle or, more specifically, the row indices of the non-zero entries in a column of the boundary matrix. Each list is sorted with the largest row index readily available at the top. Adding two such lists means merging them and removing duplicate indices. Since the lists are sorted this takes time linear in the lengths of the two lists. We store the list that represents the column j in $L[i]$, where $i = low(j)$. When $low(j)$ changes we move the list and since it can only decrease the list moves monotonically to the left. Letting i be the top index in a moving list L we encounter two cases.

`Collision::` $L[i]$ is non-empty. We add $L[i]$ to L.
`Arrival::` $L[i]$ is empty. We set $L[i]$ equal to L.

After adding $L[i]$ in the case of a collision, the top index of the list L is smaller than before and we continue the search. It is also possible that adding $L[i]$ leaves L empty. In this case we end the search and mark the simplex σ_j that initiated the search as positive. If L does not become empty it is eventually stored at some $L[i]$. We mark σ_j as negative and pair σ_i with σ_j. The number of times the list moves before reaching σ_i is at most $j - i$, the persistence of the pair. A list added to L in this search is initiated by a simplex $\sigma_{j'}$, with $\dim \sigma_{j'} = \dim \sigma_j = p$ and $j' < j$, and stored with a simplex σ_k, with $k < j'$. It can therefore not store more than $j' - k < j - k$ times $p+1$ simplices, namely the codimension one faces of all p-simplices in the interval. Assuming the dimension is a constant, the at most $j - i$ steps thus take time at most proportional to $j - i$ each. The running time of the entire algorithm is therefore at most proportional to the sum of squares of the persistences. In other words, the running time is sensitive to the output although not to the amount of output generated, which is at most n pairs. Each persistence is $j - i \leq n$ which implies the more conservative upper bound of n^3.

4. Variants

In this section we discuss variants of persistence that arise when we modify the filtration in which homology classes are tracked. After discussing relative homology we extend persistence to essential classes, which are not measured by ordinary persistence as

described in Section 2. Then, motivated by stratified spaces, we define persistence for intersection homology. Finally, we discuss how to localize generating cycles computed by the persistence algorithm using Mayer-Vietoris sequences.

Relative homology. Here the motivating application is the estimation of the dimension of an embedded manifold $\mathbb{M}$ presented to us by a finite point sample [**39**]. Letting x be a point of $\mathbb{M}$, we consider a shrinking sequence of neighborhoods of x in the ambient space. For each neighborhood we are interested in the relative homology groups and the maps induced by inclusion between the groups of different neighborhoods. If $\mathbb{M}$ is a k-dimensional manifold embedded in $\mathbb{R}^d$, $k \leq d$, we expect to see a k-dimensional relative class with large persistence. All other classes reflect the sampling within $\mathbb{M}$ and have small persistence if the sampling is sufficiently fine.

Let K be a simplicial complex and $K_l \subseteq K$ a subcomplex. Relative homology describes the connectivity of $K - K_l$, which is generally not a complex. This is done by forming chain groups of the pair, $\mathsf{C}_p(K, K_l) = \mathsf{C}_p(K)/\mathsf{C}_p(K_l)$. The effect of taking the quotient is to identify two chains that are the same in $K - K_l$ but possibly different in K. Cycle and boundary subgroups are defined as before, and their quotients are the *relative homology groups* of the pair, denoted $\mathsf{H}_p(K, K_l)$. Now let K_0 to K_m be a filtration of K as before. The inclusion $K_l \subseteq K_{l'}$ induces a homomorphism $\mathbf{g}_p^{l,l'} : \mathsf{H}_p(K, K_l) \to \mathsf{H}_p(K, K_{l'})$. A relative homology class is again born at some (K, K_l) and because the last relative homology group is empty it is guaranteed to eventually die.

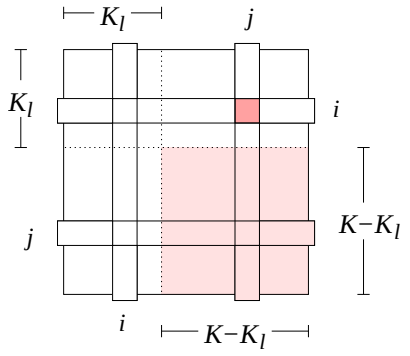

Figure 6: The relative homology groups of (K, K_l) can be read off the shaded portion of the reduced boundary matrix. If $i = low(j)$ then column i is zero and row j does not contain a lowest 1.

To compute ranks of relative homology groups and persistence pairs we use the exact same algorithm as before. The only thing different is the interpretation of the reduced matrix. Sorting the simplices as before, K_l corresponds to an upper left submatrix and $K - K_l$ to the lower right submatrix $R_{\ell r}$; see Figure 6. The rank of the relative homology group is

$$\operatorname{rank} \mathsf{H}_p(K, K_l) \quad = \quad \#Zero_p(R_{\ell r}) - \#Low_p(R_{\ell r}).$$

Recall the interpretation of $i = low(j)$ with $p = \dim \sigma_j$ in the original filtration: it represents a $(p-1)$-dimensional homology class that is born when σ_i is added and dies when σ_j is added. In the filtration of pairs the same lowest 1 represents a p-dimensional relative homology class that is born when σ_i is removed (added to K_l) and dies when σ_j

is removed. To see this we just need to observe the contribution of the lowest one to the formulas for $\mathsf{H}_p(K_l)$ and $\mathsf{H}_p(K, K_l)$ as l increases. Similarly, we observe that a $(p-1)$-dimensional essential class of K that is born at K_l exists in the relative homology groups from the beginning and dies at (K, K_l).

Extended persistence. Here the motivating application is the identification of cavities and protrusions of macromolecules for the purpose of protein docking. Inspired by the pioneering work of Connolly [**16**] we use the critical points of a function defined on the surface $\mathbb{M}$ of the macromolecule for this purpose. The particular function we have in mind is the *elevation* which was introduced in [**1**] and applied to coarse protein-protein docking in [**44**]. To define it at a given point $x \in \mathbb{M}$ we consider the height function $f : \mathbb{M} \to \mathbb{R}$ in a direction normal to $\mathbb{M}$ at x. By construction, x is a critical point of f. We apply persistence and if x gets paired with another critical point y of f then we define the elevation of x equal to $|f(x) - f(y)|$. If x does not get paired then its elevation remains undefined which is a shortcoming that would handicap the approach to docking. We thus extend persistence such that all critical points get paired, also the ones that give birth to essential cycles of $\mathbb{M}$.

We describe the extension for a d-manifold $\mathbb{M}$ and a Morse function $f : \mathbb{M} \to \mathbb{R}$ defined on it. Choose regular values $t_0 < t_1 < \ldots < t_m$ bracketing the m critical values and set $\mathbb{M}_i = f^{-1}(-\infty, t_i]$, a manifold with boundary $f^{-1}(t_i)$. We also consider the superlevel set $\mathbb{M}^{m-i} = f^{-1}[t_i, \infty)$, which has the same boundary. To define the pairing we take the ascending sequence of sublevel sets followed by the descending sequence of complements of superlevel sets. As usual, the corresponding homology groups are connected by maps induced by inclusion,

$$\begin{aligned} 0 \;=\; \mathsf{H}_p(\mathbb{M}_0) \quad &\to \ldots \to \mathsf{H}_p(\mathbb{M}_m) \\ \to \mathsf{H}_p(\mathbb{M}, \mathbb{M}^0) \;&\to \ldots \to \mathsf{H}_p(\mathbb{M}, \mathbb{M}^m) \;=\; 0. \end{aligned}$$

An essential class that is born at $\mathbb{M}_i$ is not paired by ordinary persistence but it dies in the second half of the sequence. Descending through the superlevel sets we look for the first $\mathbb{M}^{m-j}$ (the largest j) that contains a class that is homologous in $\mathbb{M}$. We then say the class dies entering $\mathbb{M}^{m-j}$ and we pair the i-th critical point with the j-th critical point.

To compute the persistence pairs we work with a triangulation K of $\mathbb{M}$ and the piecewise linear extension of f defined on its vertices. Assuming distinct function values we sort the vertices such that $f(u_1) < f(u_2) < \ldots < f(u_m)$. Letting K_l be the full subcomplex defined by the first l vertices in this ordering and L^{m-l} the full subcomplex defined by the last $m - l$ vertices, we substitute the K_l for the sublevel sets and the L^{m-l} for the superlevel sets. This gives two filtrations of K, the ascending sequence of the K_l and the descending sequence of the L^{m-l}.

The algorithm is the same as before but applied to an augmented boundary matrix, as shown in Figure 7. The upper left submatrix, A, is the boundary matrix defined by a total ordering of the simplices that is compatible with the ascending filtration. The lower right submatrix, B, is the boundary matrix defined by a total ordering of the same simplices but now compatible with the descending filtration. The upper right submatrix, P, stores the permutation that connects the two sequences. The entire matrix may be interpreted as the boundary matrix of the cone over K. After reducing the augmented boundary matrix we get lowest ones in A, B, as well as in P. The ones in A define the *ordinary* persistence pairs, same as in Section 2. The ones in B define the *relative* persistence pairs, as discussed above. The new information is in P whose lowest ones define the *extended* persistence pairs. They correspond to the homology classes that are born going up and die coming down.

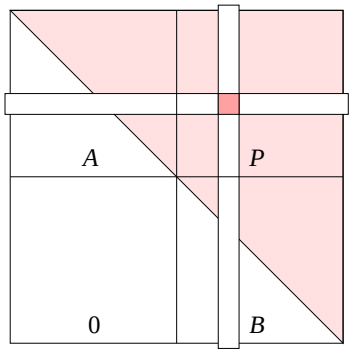

Figure 7: The augmented boundary matrix storing the ascending filtration in A, the descending filtration in B, and the connecting permutation in P. After reduction the extended persistence pairs are given by the lowest ones in P.

A crucial result about extended persistence for a Morse function is its symmetry, that is, we get the same pairing for f and for $-f$. This is important for elevation which would otherwise not be well defined. The proof of symmetry relies on Poincaré and Lefschetz duality. Indeed, the construction of the extended filtration is guided by the desire to guarantee this symmetry property. We refer to [**14**] for further details.

Intersection homology. When K is not a manifold, it no longer satisfies Poincarè duality. Extended persistence can still be defined but the duality property will no longer hold. To extend the theory, Bendich et al. use intersection homology which was developed precisely to guarantee Poincaré duality for a larger class of spaces [**4**]. We aim at using this more general theory in the reconstruction of stratified spaces from point cloud data. Recall that a *stratified space* is a topological space $\mathbb{X} \subseteq \mathbb{R}^n$ and a collection of nested subspaces

$$\emptyset = \mathbb{X}_{-1} \subset \mathbb{X}_0 \subset \mathbb{X}_1 \subset \ldots \subset \mathbb{X}_d = \mathbb{X}$$

in which the *i-stratum*, $S_i = \mathbb{X}_i - \mathbb{X}_{i-1}$, is a possibly empty i-dimensional submanifold of $\mathbb{R}^n$, and each point of S_i has a neighborhood in $\mathbb{X}$ that is a product of an i-dimensional ball in S_i with the cone on a $(d-i-1)$-dimensional stratified space. When $\mathbb{X}$ is the underlying space of a simplicial complex, we assume that each $\mathbb{X}_i$ is the underlying space of a subcomplex. A good example of a stratified space is the suspended torus, $\Sigma\mathbb{T}$, obtained by collapsing each end of the product $\mathbb{T} \times [-1, 1]$ to a point. The stratum S_0 consists of the two points, $S_1 = S_2 = \emptyset$, and S_3 is the rest. The homology of $\Sigma\mathbb{T}$ has rank 1 in dimensions 0 and 3, rank 2 in dimension 2 and is 0 otherwise, so $\Sigma\mathbb{T}$ does not satisfy Poincarè duality with ordinary homology.

Goresky and McPherson defined a new theory called *intersection homology* for stratified spaces [**30**]. The idea is that one only considers simplices that intersect the strata of $\mathbb{X}$ in a specific way. To describe what this means we use a vector $P = (p_1, p_2, \ldots, p_d)$ of integers, called a *perversity*, with $p_1 = -1$ or 0, $p_2 = 0$, and p_{i+1} equal to p_i or $p_i + 1$. A (closed) i-simplex σ is *proper* if $\dim(\sigma \cap \mathbb{X}_{d-k}) \leq i - k + p_k$, for each $k > 0$. Note that if $p_i = 0$ for all i then the condition is satisfied if each simplex meets each stratum transversally. In particular, simplices σ contained in $\mathbb{X}_{d-1}$ are necessarily improper because $\dim(\sigma \cap \mathbb{X}_{d-1}) = i > i - 1$. If some of the p_i are positive then intersections can be non-transversal and thus of dimension higher than $i - k$. An i-chain is *allowable* if it

is the sum of proper simplices and its boundary is the sum of proper simplices and simplices in $\mathbb{X}_{d-1}$. A simplex in an allowable chain may have a face that is not proper but this face must be in $\mathbb{X}_{d-1}$ or cancelled by the face of another simplex in the chain. The usual boundary map takes allowable chains to allowable chains and we define the intersection homology groups, $\mathsf{I}^P\mathsf{H}_i(\mathbb{X})$, to be the homology groups of this chain complex. The main result about these groups is that when two perversities P and Q add up to the maximum perversity, $(-1, 0, 1, \ldots, d-2)$, the corresponding intersection homology groups are dual so that $\mathsf{I}^P\mathsf{H}_i(\mathbb{X})$ is isomorphic to $\mathsf{I}^Q\mathsf{H}_{d-i}(\mathbb{X})$. For example, when $\mathbb{X} = \Sigma\mathbb{T}$ the two dual perversities $P = (0, 0, 1)$ and $Q = (-1, 0, 0)$ give us

$$\begin{aligned} \mathsf{I}^P\mathsf{H}_1(\mathbb{X}) &\simeq \mathsf{I}^Q\mathsf{H}_2(\mathbb{X}) \simeq 0; \\ \mathsf{I}^P\mathsf{H}_2(\mathbb{X}) &\simeq \mathsf{I}^Q\mathsf{H}_1(\mathbb{X}) \simeq (\mathbb{Z}/\mathbb{Z}_2)^2; \end{aligned}$$

because 2-simplices are not allowed to meet the singular points for Q but they are for P. Given a filtration of $\mathbb{X}$ that is compatible with the stratification, inclusion induces a

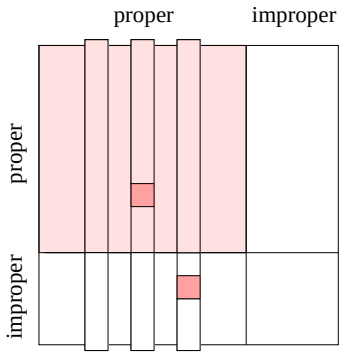

Figure 8: The reduced boundary matrix in which improper simplices are ordered to come last. From left to right the high-lighted columns represent an allowable cycle, an allowable chain, and a non-allowable chain.

natural map on intersection homology so we can define persistence in the usual way. The algorithm for computing it is the usual one once we set up the matrix as shown in Figure 8. In this matrix we reorder the simplices such that the improper ones come last. Only columns in the proper left portion of the reduced boundary matrix are relevant. If such a column has its lowest one in the improper bottom portion it corresponds to a non-allowable chain because its boundary includes an improper simplex. A column that has its lowest one in the proper top portion corresponds to an allowable chain that is negative and is paired with the proper simplex for that row. Finally, a zero column represents an allowable cycle, and is thus positive. Hence

$$\operatorname{rank} \mathsf{I}^P\mathsf{H}_p(\mathbb{X}) = \#Zero_p(R_\ell) - \#Low_p(R_{u\ell}),$$

where R_ℓ is the left submatrix defined by the columns of the proper simplices and $R_{u\ell}$ is the upper submatrix of R_ℓ defined by the rows of the proper simplices.

Localized homology. There are applications in which we are exclusively interested in local cycles or representatives of homology classes that are as local as possible. To give meaning to this notion we assume a covering of a simplicial complex K by subcomplexes

K_1 to K_m. Let $B_1 = K_1 \amalg K_2 \amalg \ldots \amalg K_m$ be the disjoint union of the subcomplexes and consider the homomorphism $\mathbf{f}_p : \mathsf{H}_p(B_1) \to \mathsf{H}_p(K)$ induced by the inclusions $K_i \subseteq K$. Zomorodian and Carlsson define the *localized homology* as the image of $\mathbf{f}_p$ and they show how to compute it with the persistence algorithm [**47**]. The main ingredient in their solution is the *Mayer-Vietoris blowup complex*, B. To define it let σ be a simplex in K and $J \subseteq \{1, 2, \ldots, m\}$ such that $\sigma \in K_i$ for each $i \in J$. Letting B_j be the set of products $\sigma \times J$ with $\operatorname{card} J \leq j$ gives a filtration

$$\emptyset = B_0 \subseteq B_1 \subseteq \ldots \subseteq B_m = B;$$

see Figure 9. Importantly, the blowup complex has the same homotopy type as the given simplicial complex, $B \simeq K$ [**42**]. To compute the localized homology we reduce the

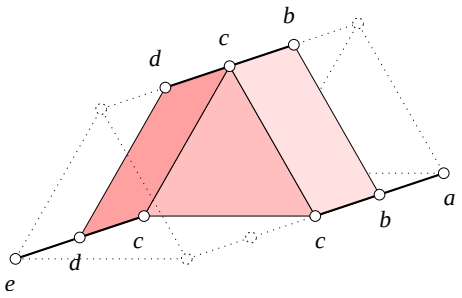

Figure 9: The blowup complex of a one-dimensional simplicial complex covered by three subcomplexes displayed along the edges of the prism.

boundary matrix D of B defined by an ordering of the simplex products that is compatible with the filtration of the B_j. The fact that we deal with simplex products instead of simplices causes no difficulties since boundaries are readily defined. The localized homology consists of the homology classes that are born in B_1 and stay alive during the entire process. To read them off the reduced boundary matrix we let $R_{1,[m]}$ and $R_{[m],1}$ be the submatrices of the reduced matrix that consist of the rows and columns corresponding to simplices in B_1. We count the zero columns and lowest ones to get

$$\operatorname{rank} \mathbf{f}_p \quad = \quad \#Zero_p(R_{[m],1}) - \#Low_p(R_{1,[m]}).$$

Indeed, the first term counts the p-dimensional homology classes born in B_1 and the second counts among them the classes killed during the construction of the blowup complex.

5. Spectral Sequences

Topologists will immediately recognize a connection between persistence and spectral sequences. We shed light on this by reviewing how spectral sequences are constructed using the algorithm in Section 3.

Diagonal sweep. Again we start with the filtration of a simplicial complex, $\emptyset = K_0 \subset K_1 \subset \cdots \subset K_m = K$. Using a compatible total ordering of the simplices we let D be the boundary matrix which we write in block form. Specifically, D_i^j records the codimension one faces of simplices in $K_j - K_{j-1}$ that lie in $K_i - K_{i-1}$. It is the intersection of a block of rows D_i and a block of columns D^j. Since the boundary matrix is upper triangular we have $D_i^j = 0$ whenever $i > j$. We reduce the boundary matrix with left-to-right column

additions, as before, but instead of sweeping the matrix from left to right we sweep it diagonally. More precisely we work in phases and in Phase r we reduce columns in D^j by adding columns in D^{j-r+1} to D^j. The columns get reduced from the diagonal outward, as illustrated in Figure 10. Since entries below the diagonal are zero this is the same as getting reduced from bottom to top.

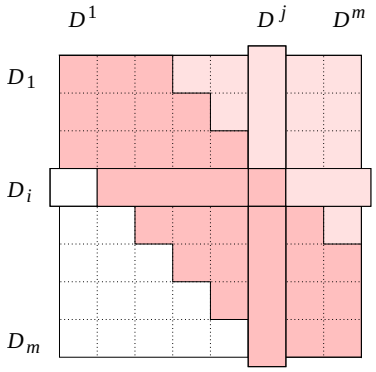

Figure 10: After three phases the triple blocks along the diagonal are reduced. The highlighted block of rows D_i and columns D^j intersect in the block matrix D_i^j.

```
for r = 1 to m do
  for j = r to m do
    take the columns ι in D^j from left to right;
    while low(ι) is in D_{j−r+1} and
          ∃ι′ < ι not to the left of D^{j−r+1}
          with low(ι′) = low(ι) ≠ 0 do
      add column ι′ to column ι
    endwhile
  endfor
endfor.
```

The result of the algorithm is the same as that of the algorithm in Section 3, only the order in which the columns are added is different. By definition, if a leftmost lowest one is in D_i^j it belongs to a simplex pair of persistence $j - i$. This algorithm thus computes the pairs in the order of non-decreasing persistence.

Groups and maps. We now interpret the diagonal sweep algorithm in terms of groups that make up the spectral sequence of the filtration. Recall the chain groups and boundary maps, $\partial : \mathsf{C}_p \to \mathsf{C}_{p-1}$, which form the chain complex defined by K. For each j we let C_p^j be the group of p-chains of $K_j - K_{j-1}$ and for each $c \in \mathsf{C}_p^j$ we let $\partial_i^j(c)$ be the sum of terms of $\partial(c)$ that lie in $K_i - K_{i-1}$. Thus $\partial_i^j : \mathsf{C}_p^j \to \mathsf{C}_{p-1}^i$ and

$$\partial(c) \quad = \quad \partial_j^j(c) + \partial_{j-1}^j(c) + \ldots + \partial_0^j(c).$$

The block D_i^j in the boundary matrix represents the maps ∂_i^j simultaneously for all dimensions. In spectral sequences we approximate ∂ by $\partial_j^j + \partial_{j-1}^j + \ldots + \partial_i^j$ for decreasing i. The spectral sequence itself consists of a collection of groups $\mathsf{E}_{p,q}^r$ and maps $\mathbf{d}_{p,q}^r$ between

them. We follow the customary convention in which the first subscript, p, identifies the block of columns, the sum of subscripts, $p+q$, gives the dimension, and the superscript, r, counts the phases in the iteration. To begin let $\mathsf{E}^0_{p,q} = \mathsf{C}^p_{p+q}$ and let $\mathbf{d}^0_{p,q} : \mathsf{E}^0_{p,q} \to \mathsf{E}^0_{p,q-1}$ be defined by the $(p+q)$-dimensional boundary map restricted to D^p_p, that is, $\mathbf{d}^0_{p,q}$ is ∂^p_p as applied to $(p+q)$-chains. It is easy to check that $\mathbf{d}^0_{p,q-1} \circ \mathbf{d}^0_{p,q} = 0$ so we get a set of vertical chain complexes which we write in a grid:

$$\begin{array}{cccc}
\cdots & \cdots & \cdots & \cdots \\
\downarrow & \downarrow & \downarrow & \downarrow \\
\mathsf{E}^0_{1,1} & \mathsf{E}^0_{2,1} & \mathsf{E}^0_{3,1} & \cdots \\
\downarrow & \downarrow & \downarrow & \downarrow \\
\mathsf{E}^0_{1,0} & \mathsf{E}^0_{2,0} & \mathsf{E}^0_{3,0} & \cdots \\
\downarrow & \downarrow & \downarrow & \downarrow \\
\mathsf{E}^0_{1,-1} & \mathsf{E}^0_{2,-1} & \mathsf{E}^0_{3,-1} & \cdots \\
 & \downarrow & \downarrow & \downarrow \\
 & \mathsf{E}^0_{2,-2} & \mathsf{E}^0_{3,-2} & \cdots \\
 & & \downarrow & \downarrow \\
 & & \mathsf{E}^0_{3,-3} & \cdots \\
 & & & \downarrow \\
 & & & \cdots
\end{array}$$

We call this the E^0-*term* of the spectral sequence. The groups $\mathsf{E}^0_{p,q}$ are generated by the columns in D^p and the maps $\mathbf{d}^0_{p,q}$ are represented by the block D^p_p.

Iteration. After interpreting the original boundary matrix we now push this interpretation through the phases of the algorithm. For the first phase, we take the homology of the above vertical complexes and define

$$\mathsf{E}^1_{p,q} \quad = \quad \ker \mathbf{d}^0_{p,q} / \operatorname{im} \mathbf{d}^0_{p,q+1}.$$

An element of $\mathsf{E}^1_{p,q}$ is thus the equivalence class of a chain $c \in \mathsf{C}^p_{p+q}$ with $\partial^p_p(c) = 0$, where two chains are equivalent if their difference lies in the image of ∂^p_p, taking of course the boundary map that applies to chains of one higher dimension. In other words, the element is a relative homology class and more generally $\mathsf{E}^1_{p,q} \simeq \mathsf{H}_{p+q}(K_p, K_{p-1})$. Representatives of $\mathsf{E}^1_{p,q}$ are computed by reducing the matrix D^p_p, which is what the diagonal sweep algorithm does in Phase $r = 1$. The zero columns in D^p_p correspond to positive simplices and represent cycles. Some are paired and have zero persistence since their classes come and go within $K_p - K_{p-1}$. Others are not paired and their cycles are the generators of $\mathsf{E}^1_{p,q}$. Next we define $\mathbf{d}^1_{p,q} : \mathsf{E}^1_{p,q} \to \mathsf{E}^1_{p-1,q}$. Letting γ be a class in $\mathsf{E}^1_{p,q}$ we set $\mathbf{d}^1_{p,q}(\gamma)$ equal to the equivalence class of $\partial^{p-1}_p(\gamma)$ in $\mathsf{E}^1_{p-1,q}$. This gives a set of horizontal chain complexes which we write in a grid as before:

$$\begin{array}{ccccccc}
\cdots & \leftarrow & \cdots & \leftarrow & \cdots & \leftarrow & \cdots \\
\mathsf{E}^1_{1,1} & \leftarrow & \mathsf{E}^1_{2,1} & \leftarrow & \mathsf{E}^1_{3,1} & \leftarrow & \cdots \\
\mathsf{E}^1_{1,0} & \leftarrow & \mathsf{E}^1_{2,0} & \leftarrow & \mathsf{E}^1_{3,0} & \leftarrow & \cdots \\
\mathsf{E}^1_{1,-1} & \leftarrow & \mathsf{E}^1_{2,-1} & \leftarrow & \mathsf{E}^1_{3,-1} & \leftarrow & \cdots \\
 & & \mathsf{E}^1_{2,-2} & \leftarrow & \mathsf{E}^1_{3,-2} & \leftarrow & \cdots \\
 & & & & \mathsf{E}^1_{3,-3} & \leftarrow & \cdots
\end{array}$$

This is the E^1*-term* of the spectral sequence. We take one more step before appealing to induction, taking the homology of the horizontal complexes,

$$\mathsf{E}^2_{p,q} \quad = \quad \ker \mathbf{d}^1_{p,q} / \operatorname{im} \mathbf{d}^1_{p+1,q}.$$

An element of $\mathsf{E}^2_{p,q}$ is the equivalence class of the sum of a chain $c \in \mathsf{C}^p_{p+q}$ and another chain $c' \in \mathsf{C}^{p-1}_{p+q}$. The chains satisfy $\partial^p_p(c) = 0$ and $\partial^p_{p-1}(c) + \partial^{p-1}_{p-1}(c') = 0$ and being equivalent means that the difference lies in $\operatorname{im} \partial^p_p + \operatorname{im} \partial^p_{p-1} + \operatorname{im} \partial^{p-1}_{p-1}$. The group $\mathsf{E}^2_{p,q}$ is not a relative homology group by itself but a subgroup of one, namely $\mathsf{E}^2_{p,q} \oplus \mathsf{E}^1_{p-1,q+1} \simeq \mathsf{H}_{p+q}(K_p, K_{p-2})$. Representatives of $\mathsf{E}^2_{p,q}$ are computed by reducing the double block of matrices D^p_p, D^{p-1}_{p-1}, D^{p-1}_p, D^p_{p-1}. The first two have already been reduced and the third is zero. Phase $r = 2$ completes the reduction of the double block for the remaining fourth matrix. Next we define $\mathbf{d}^2_{p,q} : \mathsf{E}^2_{p,q} \to \mathsf{E}^2_{p-2,q+1}$ which gives another set of chain complexes.

The process continues and for general phase numbers r the map takes r steps to the left and $r-1$ steps up, $\mathbf{d}^r_{p,q} : \mathsf{E}^r_{p,q} \to \mathsf{E}^r_{p-r,q+r-1}$. This gives a set of chain complexes and we take homology to enter the next phase. Since K is finite the maps are eventually zero and the sequence converges to a limit term, $\mathsf{E}^r = \mathsf{E}^\infty$ for r large enough. The homology groups of K are obtained by taking direct sums along the diagonals in the limit term. Here it is crucial that we work over a field. Over $\mathbb{Z}$, for example, there are extension problems to solve because of torsion [**5**].

6. Stability

An important property of persistence is its stability under perturbations. After formulating this concept for continuous functions, we list some of its consequences, which includes inequalities for the curvature of smooth curves and surfaces. The stability leads to continuous images, called vineyards, that track topological features in homotopies, a new paradigm in the study of dynamic processes.

Bottleneck distance. Let $\mathbb{X}$ be a topological space with two tame functions $f, g : \mathbb{X} \to \mathbb{R}$. We recall that this entails that f and g are continuous, that all sublevel sets have homology groups of finite rank, and that these groups change at a finite number of homological critical values. As explained in Section 2, we encode the homology groups of the sublevel sets in the persistence diagrams $\operatorname{Dgm}_p(f)$ and $\operatorname{Dgm}_p(g)$, each a multiset of points in the extended plane, $\bar{\mathbb{R}}^2$. The L_∞-distance between points $u = (u_1, u_2)$ and $v = (v_1, v_2)$ in the extended plane is $\|u - v\|_\infty = \max\{|u_1 - v_1|, |u_2 - v_2|\}$, where the difference between two infinite coordinates is defined to be zero. Given a bijection η between two diagrams, we take the supremum L_∞-distance between matched points and define the *bottleneck distance* by taking the infimum over all supremums,

$$d_B(\operatorname{Dgm}_p(f), \operatorname{Dgm}_p(g)) \quad = \quad \inf_\eta \sup_x \|x - \eta(x)\|_\infty.$$

Besides the finitely many off-diagonal points, each diagram includes copies of all points on the diagonal. These are needed for the bijections because the number of off-diagonal points in two diagrams is not necessarily the same. As suggested by Figure 11, we may think of a diagonal point as an anti-cancellation in waiting. Measuring the distance between functions by taking the supremum of the absolute difference between corresponding values, $\|f - g\|_\infty = \sup_{x \in \mathbb{X}} |f(x) - g(x)|$ we are now ready to state in what sense persistence is stable.

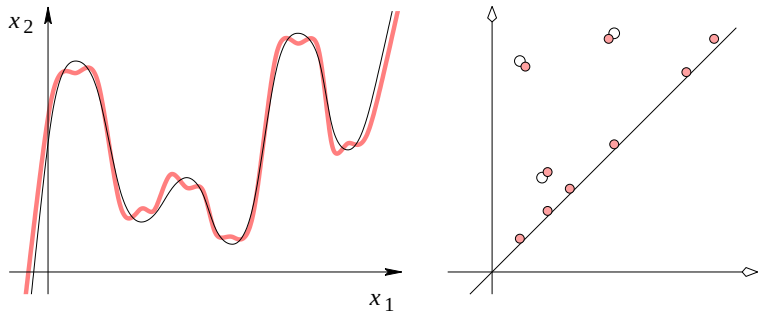

Figure 11: Left: two functions with small L_∞-distance. Right: the corresponding two persistence diagrams with small bottleneck distance.

THEOREM 6.1. *Let $\mathbb{X}$ be a topological space with tame functions $f, g : \mathbb{X} \to \mathbb{R}$. Then for each dimension p the bottleneck distance between the dimension p persistence diagrams is bounded from above by the difference between the functions, $d_B(\mathrm{Dgm}_p(f), \mathrm{Dgm}_p(g)) \leq \|f - g\|_\infty$.*

The proof given in [**13**] chases diagrams formed by homomorphisms induced by inclusions between various sublevel sets of f and g. An alternative elementary proof of a slightly weaker version of the theorem can be found in [**15**]. A proof for connected components tracked by the dimension 0 persistence diagram has independently been obtained in [**3**].

Applications. The stability of persistence diagrams has a number of consequences, some immediate and some less direct. We restrict ourselves to brief descriptions and a small number of references.

Homology inference. Let $X_0 \subseteq \mathbb{R}^d$ be a closed set and write $d_0 : \mathbb{R}^d \to \mathbb{R}$ for the Euclidean distance function that maps each point to its Euclidean distance from the nearest point in X_0. For each $\varepsilon \geq 0$, the *parallel body* is a sublevel set of the distance function, $X_0^\varepsilon = d_0^{-1}[0, \varepsilon]$. Let X_1 be another closed set in $\mathbb{R}^d$. The *Hausdorff distance* between the two sets, $d_H(X_0, X_1)$, is the infimum over all ε for which $X_0 \subseteq X_1^\varepsilon$ and $X_1 \subseteq X_0^\varepsilon$. The *homological feature size* of X_0, denoted $hfs(X_0)$, is the infimum of the positive homological critical value of d_0. Let $d_H(X_0, X_1) < \varepsilon < hfs(X_0)/4$ and $\delta > 0$ sufficiently small. Then the rank of the p-dimensional homology group of the parallel body defined by δ is

$$\operatorname{rank} \mathsf{H}_p(X_0^\delta) \quad = \quad \operatorname{rank} \operatorname{im} \mathbf{f}_\varepsilon^{3\varepsilon}, \tag{6.1}$$

where $\mathbf{f}_\varepsilon^{3\varepsilon} : \mathsf{H}_p(X_1^\varepsilon) \to \mathsf{H}_p(X_1^{3\varepsilon})$ is induced by inclusion. For example X_0 could be a body bounded by a smooth surface and X_1 could be a finite point sample of the body. In this case the homological feature size is necessarily positive and the result says that we can compute the homology of the body from a finite sample. In [**13**] this result is proved as a corollary to the stability theorem. It has been obtained independently in [**11**]. A similar result with a stronger requirement on the closeness between X_0 and X_1 can be found in [**38**].

Shape comparison. An important problem in practice is measuring the similarity between shapes, may it be faces, teeth, plants, tools, or what have you. For $i = 0, 1$ let $X_i \subseteq \mathbb{R}^3$ and $d_i : \mathbb{R}^3 \to \mathbb{R}$ the corresponding distance function on the ambient space. The difference between two distance functions is bounded from above by the Hausdorff distance between the shapes,

$$\|d_0 - d_1\|_\infty \quad \leq \quad d_H(X_0, X_1).$$

Theorem 6.1 thus implies that the bottleneck distance between corresponding persistence diagrams is bounded from above by the Hausdorff distance. We remark that the reverse is generally not true. For example, if X_1 is the mirror image of the non-symmetric shape X_0 then the two corresponding distance functions have identical persistence diagrams even though the Hausdorff distance between the two shapes is non-zero.

A finer function aimed at measuring the difference between smooth surfaces has been introduced in [**7**]. It maps each point and unit tangent vector at the point to the corresponding absolute normal curvature. This is a function over the (four-dimensional) tangent bundle of the surface. If $\eta : \mathbb{R}^3 \to \mathbb{R}^3$ is a diffeomorphism that has derivatives up to second order close to the identity then the bottleneck distance between the persistence diagrams for the surfaces X and $\eta(X)$ is small [**13**].

Curvature of curves. Let $\gamma : \mathbb{S}^1 \to \mathbb{R}^2$ be a smooth closed curve. Writing $\kappa(s)$ for the (absolute) curvature at $\gamma(s)$, the *total curvature* is

$$k(\gamma) \quad = \quad \frac{\ell(\gamma)}{2\pi} \int_{s \in \mathbb{S}^1} \kappa(s)\, \mathrm{d}s,$$

where $\ell(\gamma)$ is the length. Note that $k(\gamma)$ is also the distance traveled by the unit tangent vector on the circle of directions. Fáry's Theorem states that if the image of γ is contained in the unit disk then the total curvature cannot be less than the length, $\ell(\gamma) \leq k(\gamma)$ [**28**]. Using Theorem 6.1, [**12**] generalizes this to a statement about two smooth curves $\gamma_0, \gamma_1 : \mathbb{S}^1 \to \mathbb{R}^2$. The *Fréchet distance* between them is $d_F(\gamma_0, \gamma_1) = \inf_\varphi \sup_s \|\gamma_0(s) - \gamma_1(s)\|$, where φ ranges over all homeomorphisms between two unit circles and s ranges over all points of the first unit circle. Letting $\ell_i = \ell(\gamma_i)$ be the length and $k_i = k(\gamma_i)$ the total curvature, we have

$$|\ell_0 - \ell_1| \quad \leq \quad [k_0 + k_1 - 2\pi]\, d_F(\gamma_0, \gamma_1). \tag{6.2}$$

Letting γ_0 be the curve inside the unit disk and γ_1 a tiny circle around the origin we see that this inequality indeed implies Fáry's Theorem in the plane. Both Fáry's Theorem and (6.2) generalize to smooth curves in Euclidean spaces of dimension beyond two.

Curvature of surfaces. There is a similar inequality that relates two notions of curvature of a closed surface X embedded in $\mathbb{R}^3$. Letting $\kappa_1(x) \geq \kappa_2(x)$ be the principal curvatures at a point $x \in X$, the *total mean curvature* and the *total absolute Gaussian curvature* of the surface are

$$\begin{aligned} h(X) \quad &= \quad \frac{1}{2} \int_{x \in X} (\kappa_1(x) + \kappa_2(x))\, \mathrm{d}x; \\ k(X) \quad &= \quad \int_{x \in X} |\kappa_1(x)\kappa_2(x)|\, \mathrm{d}x. \end{aligned}$$

Since it is embedded the surface necessarily partitions $\mathbb{R}^3$ into the bounded set $\bar{X}$ of points on and inside X and the unbounded complement of $\bar{X}$. Given two surfaces X_i with total

mean curvature $h_i = h(X_i)$ and total absolute Gaussian curvature $k_i = k(X_i)$, for $i = 0, 1$, we have

$$|h_0 - h_1| \quad \leq \quad [k_0 + k_1 - 4\pi(1+g)]\, d_F(\bar{X}_0, \bar{X}_1), \tag{6.3}$$

where g is the common genus of X_0 and X_1 and d_F is the Fréchet distance between the bodies bounded by the surfaces. Recall that this distance is the supremum of $\|x - \eta(x)\|$ over all points $x \in \bar{X}_0$ and all homeomorphisms $\eta : \bar{X}_0 \to \bar{X}_1$. The latter exist because the surfaces have the same genus. The proof of the inequality given in [**12**] uses integral geometry expressions of the total mean curvature and the total absolute Gaussian curvature. These formulations extend naturally to non-smooth surfaces. The inequality can thus be used to bound the difference between the total mean curvature of a smooth surface and a piecewise linear approximation of that surface.

Time series. So far we have only discussed persistence for single functions. We now consider how persistence changes when we have a 1-parameter family of functions. In this case the points in the persistence diagrams move in the plane. Sometimes a point appears or disappears and sometimes two points interact in what we will call a switch. Theorem 6.1 limits the changes to continuous motion. The diagrams can therefore be stacked up to form a collection of curves. We explain this in some detail assuming a d-manifold $\mathbb{M}$ and two Morse functions $f_0, f_1 : \mathbb{M} \to \mathbb{R}$. Any two smooth functions can be connected by the straight-line homotopy and therefore also f_0 and f_1. In other words, there is a smooth homotopy $F : \mathbb{M} \times [0,1] \to \mathbb{R}$ with $F(x,0) = f_0(x)$ and $F(x,1) = f_1(x)$ for all $x \in \mathbb{M}$. The thus defined path consists of functions $f_t(x) = F(x,t)$ for t from 0 to 1. Furthermore, the path can be deformed slightly to a *generic path* in which every f_t is Morse except at a finite number of times $0 < t_1 < \ldots < t_n < 1$ at which either

- two critical points of f_{t_i} share the same critical value;
- a critical point x is degenerate with nearby local coordinates under which f_{t_i} takes the form $f_{t_i}(y) = f_{t_i}(x) + y_1^3 \pm y_2^2 \pm \ldots \pm y_d^2$;

see [**10**]. The first violation is an *interchange* of two critical values. The degenerate critical point in the second violation is known as a *birth-death point*: as f_t passes through f_{t_i} two non-degenerate critical points annihilate each other in a cancellation at x (a *death*) or two non-degenerate critical points emerge in an anticancellation from x (a *birth*).

As we follow the generic path of functions the persistence diagram changes in interesting ways. As long as the function remains Morse the pairing of critical points does not change and the off-diagonal points in the diagrams vary continuously. At a death an off-diagonal point merges into the diagonal while at a birth one emerges from the diagonal. At an interchange there are two possibilities depending on whether the pairing changes. Suppose x_t and y_t are two critical points that go through an interchange at $t = t_i$ and before the interchange x_t is paired with x'_t and y_t is paired with y'_t. Assuming x_t and y_t are both positive the points in the diagrams that represent the pairs are $u_t = (f_t(x_t), f_t(x'_t))$ and $v_t = (f_t(y_t), f_t(y'_t))$. At $t = t_i$ the two points line up on a common vertical line. There are now two possibilities. In one case the pairs remain unchanged and the points u_t and v_t simply pass one another. In the other case the pairing *switches* by which we mean that for $t > t_i$ the points continue on the trajectories $u_t = (f_t(y_t), f_t(x'_t))$ and $v_t = (f_t(x_t), f_t(y'_t))$. Since the switch happens at the moment u_t and v_t share the same first coordinate there is no jump although the speed and direction of the two points undergoes a sudden change. We use the types of x_t and y_t to distinguish between three kinds of switches. It is easy to see that a necessary condition for a switch is that the interchanging critical points have the same index. We get another, less obvious necessary condition by

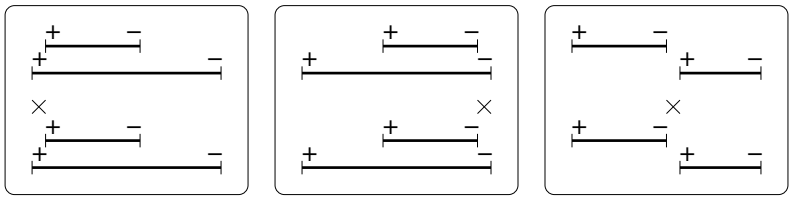

Figure 12: From left to right: a switch between two positive critical points, between two negative critical points, and between a positive and a negative critical point. In the third case the two interchanging critical points also swap their types.

interpreting the points u_t and v_t as two intervals. As proved in [**15**] a switch requires that both before and after the switch the two intervals are nested or disjoint; see Figure 12.

We can track the evolution of the persistence diagram by adding an extra dimension for time. The *vineyard* is the collection of points $(f_t(x_t), f_t(x'_t), t)$ where the (x_t, x'_t) are critical points paired by persistence. The above analysis shows that the vineyard is a family of curves that start and end either at off-diagonal locations in the planes $t = 0, 1$ or on the diagonal wall of points (x, x, t).

Dynamic algorithm. To compute the vineyard of the family f_t we use a triangulation K of the manifold and a filtration that changes with t. Interchanges, deaths, and births all reduce to transpositions in the compatible ordering of simplices. Such a transposition may or may not affect the pairing of simplices. Writing n for the number of simplices, the algorithm in [**15**] takes time O(n) to decide which case it is and to update the pairing if it is affected by the transposition. To describe the algorithm we let D be the boundary matrix defined by the ordering of the simplices at time t. Letting R be a corresponding reduced boundary matrix we have $R = DV$, and since V is invertible we have $D = RU$, where $U = V^{-1}$. We call this an *RU-decomposition* of D assuming R is reduced and U is upper triangular. The RU-decomposition is not unique but any one defines the same pairing of simplices. To transpose two simplices in the ordering we swap the corresponding rows and columns in D. Equivalently, we multiply D with the permutation matrix from both sides giving $PDP = (PRP)(PUP)$. It fails to be an RU-decomposition if PRP is not reduced or PUP is not upper triangular. Both shortcomings can be remedied with a constant number of row and column operations giving an algorithm that takes linear time per transposition in the worst case; see [**15**] for details.

In practice it is more efficient to represent both R and U as sparse matrices. To efficiently maintain the pairing requires a slightly richer collection of primitives than computing the pairing. We therefore need a sparse matrix data structure that is different from the one described in Section 3. To represent R we use two linear arrays, a vertical one to index the rows and a horizontal one to index the columns. Each column is represented by a singly linked list storing the row numbers of its non-zero entries, as sketched in Figure 13. To add two columns we merge the two linked lists while deleting nodes that come in duplicate. To swap two columns we swap two pointers in the horizontal array. To swap two rows we record the new row positions in the vertical array but do not propagate that change to the linked lists. This way the lists remain consistently ordered which simplifies the merging since it can be done without reordering. We use a symmetric sparse matrix

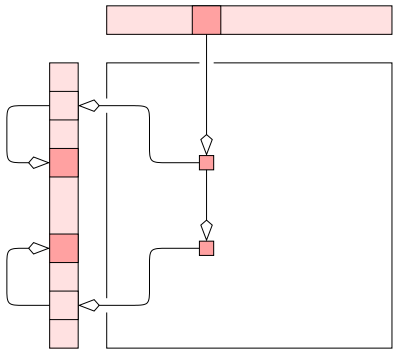

Figure 13: The sparse matrix representation of R supports column additions as well as column and row swaps.

implementation for U and get a data structure that takes a constant amount of memory per non-zero entry in R and in U.

7. Discussion

In spite of its short history, persistent homology has already lead to a number of interesting results and connected problems from seemingly distant fields. To substantiate this view we briefly mention developments that are related to persistence and we draw a speculative bigger picture by expressing where we believe persistent homology might lead us.

Related developments. We discuss three research directions: the decomposition and simplification of functions, data analysis and witness complexes, and coverage questions for sensor networks.

Morse-Smale complexes and simplification. A Morse function on a Riemannian manifold defines a gradient flow that can be used to decompose the manifold into regions of constant origin or destination. An additional non-degeneracy condition leads to Morse-Smale functions which can be used to decompose the manifold into regions of points with common origin *and* common destination. Both decompositions have applications in medical imaging [**41**] and in geometric modeling [**20**]. A show stopper in these applications is the over-segmentation resulting from spurious critical points created by noisy data or artifacts of the data representation. There has been work on simplifying the decomposition using persistent homology for 2-manifolds [**22**] and for 3-manifolds [**21**]. Both methods simplify the decomposition but do not adjust the function that leads to the simplification, which is a more difficult problem. A controlled adjustment of a piecewise linear function on a 2-manifold that simplifies the persistence diagram by eliminating points of persistence below a given threshold while retaining all other points unchanged has been described in [**25**]. The problem for manifolds of dimension three and higher is still open.

Data analysis and witness complexes. Generalizing a topology preserving network construction in [**33**], de Silva and Carlsson introduced *witness complexes* by using the majority of the data as witnesses that support the construction of simplices connecting a minority of the data points [**18**]. While there are distinct similarities to other shape reconstruction

methods, see e.g. [**2**], there are also important differences. Perhaps the most significant difference is the liberation from the metric of the ambient space. Indeed many data sets of interest are preferably interpreted as sampled from or nearby subspaces of positive codimension. Without knowing what these subspaces are, the partition of the data into landmarks and witnesses allows us to approximate distances in these subspaces. This liberation favors the use of coarse landmark sets and permits the exploration of high dimensions. At the same time, it suggests we focus on the gross, topological features of the data rather than on the fine, geometric distinctions. A good example of this research is the analysis of image data leading to the realization that small patches are located on or nearby a hypothetical Klein bottle [**8**].

Coverage of sensor networks. Here the central problem is deciding whether a collection of relatively primitive sensors with limited domains of observation cover a given region. De Silva and Ghrist use Vietoris-Rips complexes and their homology to decide this question under rather weak assumptions on what we know about the location of the sensors [**19**]. These complexes are upward completions of edge skeleta. In Euclidean space the difference between the Vietoris-Rips complex and the Čech complex (the nerve of the spherical neighborhoods) can be quantified and related to the radius of the neighborhoods. This leads to the characterization of coverage in terms of the homology of complexes. Using persistence these characterizations can be made robust to fluctuations in the distribution of sensors and gaps in the coverage.

Future directions. There are many open questions raised by our current understanding of persistent homology. One of the most important is the extent to which this theory can be generalized to a multi-variate situation in which two or more functions characterize the data. Negative results in this direction can be found in [**9**]. Questions on a different scale level are about the relationship between persistence and other broad approaches to problems in the sciences. We feel that any attempts to answer them would be premature but making the question specific might be productive.

Statistics. How different is the approach with persistent homology to high-dimensional data analysis from methods in statistics? We think there is a latent symbiotic relationship. The probabilistic aspects of persistence have not yet been explored and similarly persistence has not yet been integrated in statistical approaches to data.

Machine learning. A related question is about the connection between persistent homology and machine learning. Manifold learning is very much part of that discipline and obviously connects to topological ideas and questions of robustness addressed by persistence.

Dynamical systems. It would be interesting to extend persistence from gradient fields to general smooth vector fields defined on manifolds. We refer to [**35**] for an account of discrete methods and combinatorial algorithms in the field. The connection to the idea of persistence is still unclear.

References

[1] P. K. AGARWAL, H. EDELSBRUNNER, J. HARER AND Y. WANG. Extreme elevation on a 2-manifold. *Discrete Comput. Geom.* **36** (2006), 553–572.

[2] N. AMENTA AND M. BERN. Surface reconstruction by Voronoi filtering. *Discrete Comput. Geom.* **22** (1999), 481–504.

[3] M. D'AMICO, P. FROSINI AND C. LANDI. Optimal matching between reduced size functions. *Tech. Report no. 35, DISMI, Università di Modena e Reggio Emilia* (2003).

[4] P. BENDICH, J. HARER AND H. KING. Persistent intersection homology for stratified spaces. Manuscript, Math. Dept., Duke Univ., Durham, North Carolina, 2007.
[5] K. S. BROWN. *Cohomology of Groups.* Springer-Verlag, New York, 1994.
[6] F. CAGLIARI, M. FERRI AND P. POZZI. Size functions from the categorical viewpoint. *Acta Appl. Math.* **67** (2001), 225–235.
[7] G. CARLSSON, A. COLLINS, L. GUIBAS AND A. ZOMORODIAN. Persistence barcodes for shapes. *Internat. J. Shape Modeling* (2005).
[8] G. CARLSSON, T. ISHKHANOV, V. DE SILVA AND A. ZOMORODIAN. On the local behavior of spaces of natural images. *Internat. J. Comput. Vision*, to appear.
[9] G. CARLSSON AND A. ZOMORODIAN. The theory of multidimensional persistence. *In* "Proc. 23rd Ann. Sympos. Comput. Geom., 2007", to appear.
[10] J. CERF. La stratification naturelle des espaces de fonctions différentiables réelles et le théorème de la pseudo-isotopie. *Inst. Hautes Études Sci. Publ. Math.* **39** (1970), 5–173.
[11] F. CHAZAL AND A. LIEUTIER. Weak feature size and persistent homology: computing homology of solids in $\mathbb{R}^n$ from noisy point samples. *In* "Proc. 21st Ann. Sympos. Comput. Geom., 2005", 255–262.
[12] D. COHEN-STEINER AND H. EDELSBRUNNER. Inequalities for the curvature of curves and surfaces. *In* "Proc. 21st Ann. Sympos. Comput. Geom., 2005", 272–277.
[13] D. COHEN-STEINER, H. EDELSBRUNNER AND J. HARER. Stability of persistence diagrams. *Discrete Comput. Geom.* **37** (2007), 103–120.
[14] D. COHEN-STEINER, H. EDELSBRUNNER AND J. HARER. Extending persistence using Poincaré and Lefschetz duality. *Found. Comput. Math.*, to appear.
[15] D. COHEN-STEINER, H. EDELSBRUNNER AND D. MOROZOV. Vines and vineyards by updating persistence in linear time. *In* "Proc. 22nd Ann. Sympos. Comput. Geom., 2006", 119–126.
[16] M. L. CONNOLLY. Shape complementarity at the hemo-globin albl subunit interface. *Biopolymers* **25** (1986), 1229–1247.
[17] C. J. A. DELFINADO AND H. EDELSBRUNNER. An incremental algorithm for Betti numbers of simplicial complexes on the 3-sphere. *Comput. Aided Geom. Design* **12** (1995), 771–784.
[18] V. DE SILVA AND G. CARLSSON. Topological estimation using witness complexes. *In* "Proc. Sympos. Point-Based Graphics, 2004", 157–166.
[19] V. DE SILVA AND R. GHRIST. Coverage in sensor networks via persistent homology. *J. Alg. Geom. Topology*, to appear.
[20] H. EDELSBRUNNER. Surface tiling with differential topology. *In* "Proc. 3rd Ann. Sympos. Geom. Process., 2006", 9–11.
[21] H. EDELSBRUNNER AND J. HARER. The persistent Morse complex segmentation of a 3-manifold. Report rgi-tech-04-066, Geomagic, Research Triangle Park, North Carolina, 2004.
[22] H. EDELSBRUNNER, J. HARER AND A. ZOMORODIAN. Hierarchical Morse-Smale complexes for piecewise linear 2-manifolds. *Discrete Comput. Geom.* **30** (2003), 87–107.
[23] H. EDELSBRUNNER, D. G. KIRKPATRICK AND R. SEIDEL. On the shape of a set of points in the plane. *IEEE Trans. Inform. Theory* **IT-29** (1983), 551–559.
[24] H. EDELSBRUNNER, D. LETSCHER AND A. ZOMORODIAN. Topological persistence and simplification. *Discrete Comput. Geom.* **28** (2002), 511–533.
[25] H. EDELSBRUNNER, D. MOROZOV AND V. PASCUCCI. Persistence-sensitive simplification of functions on 2-manifolds. *In* "Proc. 22th Ann. Sympos. Comput. Geom., 2006", 127–134.
[26] H. EDELSBRUNNER AND E. P. MÜCKE. Three-dimensional alpha shapes. *ACM Trans. Graphics* **13** (1994), 43–72.
[27] H. EDELSBRUNNER AND A. ZOMORODIAN. Computing linking numbers of a filtration. *Homology, Homotopy and Applications* **5** (2003), 19–37.
[28] I. FÁRY. Sur certaines inégalités géométriques. *Acta Sci. Math. Szeged* **12** (1950), 117–124.
[29] P. FROSINI AND C. LANDI. Size theory as a topological tool for computer vision. *Pattern Recognition and Image Analysis* **9** (1999), 596–603.
[30] M. GORESKY AND R. MACPHEARSON. Intersection homology I. *Topology* **19** (1982), 135–162.
[31] A. HATCHER. *Algebraic Topology.* Cambridge Univ. Press, England, 2002.
[32] R. KANNAN AND A. BACHEM. Polynomial algorithms for computing the Smith and Hermite normal forms of an integer matrix. *SIAM J. Comput.* **8** (1979), 499–507.
[33] T. MARTINETZ AND K. SCHULTEN. Topology representing networks. *Neural Networks* **7** (1994), 507–522.
[34] J. MILNOR. *Morse Theory.* Princeton Univ. Press, New Jersey, 1963.
[35] T. KACZYNSKI, K. MISCHAIKOW AND M. MROZEK. *Computational Homology.* Springer-Verlag, New York, 2004.

[36] D. MOROZOV. Persistence algorithm takes cubic time in worst case. BioGeometry News, Dept. Comput. Sci., Duke Univ., Durham, North Carolina, 2005.
[37] J. R. MUNKRES. *Elements of Algebraic Topology.* Addison-Wesley, Redwood City, California, 1984.
[38] P. NIYOGI, S. SMALE AND S. WEINBERGER. Finding the homology of submanifolds with high confidence from random samples. Report TR-2004-08, Dept. Comput. Sci., Univ. Chicago, Illinois, 2004.
[39] E. RANNAUD. Persistence in computational topology. Manuscript, Math. Dept., Stanford Univ., California, 2004.
[40] V. ROBINS. Toward computing homology from finite approximations. *Topology Proceedings* **24** (1999), 503–532.
[41] J. ROERDINK AND A. MEIJSTER. The watershed transform: definitions, algorithms, and parallelization strategies. *Fundamenta Informaticae* **41** (2000), 187–228.
[42] G. SEGAL. Classifying spaces and spectral sequences. *Inst. Hautes Études Sci. Publ. Math.* **34** (1968), 105–112.
[43] A. STORJOHANN. Near optimal algorithms for computing Smith normal forms of integer matrices. *In* "Proc. ACM Sympos. Symbolic Algebraic Comput. 1996", 267–274.
[44] Y. WANG, P. K. AGARWAL, P. BROWN, H. EDELSBRUNNER AND J. RUDOLPH. Coarse and reliable geometric alignment for protein docking. *In* "Proc. Pacific Sympos. Biocomput., 2005", 65–75.
[45] A. ZOMORODIAN. *Topology for Computing.* Cambridge Univ. Press, England, 2005.
[46] A. ZOMORODIAN AND G. CARLSSON. Computing persistent homology. *Discrete Comput. Geom.* **33** (2005), 249–274.
[47] A. ZOMORODIAN AND G. CARLSSON. Localized homology. *In* "Shape Modeling Internat., 2007", to appear.

DEPARTMENTS OF COMPUTER SCIENCE AND OF MATHEMATICS, DUKE UNIVERSITY, DURHAM, AND GEOMAGIC, RESEARCH TRIANGLE PARK, NORTH CAROLINA, USA.
E-mail address: edels@cs.duke.edu

DEPARTMENTS OF MATHEMATICS AND SECTION IN COMPUTATIONAL BIOLOGY AND BIOINFORMATICS, DUKE UNIVERSITY, DURHAM, NORTH CAROLINA, USA.
E-mail address: harer@math.duke.edu